



3D-QSAR and 3D-QSSR models of negative allosteric modulators facilitate the design of a novel selective antagonist of human $\alpha 4\beta 2$ neuronal nicotinic acetylcholine receptors

Brandon J. Henderson^{a,*}, Crina M. Orac^b, Iwona Maciagiewicz^b, Stephen C. Bergmeier^b, Dennis B. McKay^a

^a Division of Pharmacology, College of Pharmacy, The Ohio State University, Columbus, OH (BJH, DBM), USA

^b Department of Chemistry and Biochemistry, Ohio University, Athens, OH (CMO, IM, SCB), USA

ARTICLE INFO

Article history:

Received 3 October 2011
Revised 11 November 2011
Accepted 14 November 2011
Available online 20 November 2011

Keywords:

Structure–activity relationship (SAR)
Qualitative structure–activity relationship (QSAR)
Qualitative structure selectivity relationship (QSSR)
Nicotinic acetylcholine receptor (nAChR)
 $\alpha 4\beta 2$
 $\alpha 3\beta 4$
Negative allosteric modulator (NAM)

ABSTRACT

Subtype selective molecules for $\alpha 4\beta 2$ neuronal nicotinic acetylcholine receptors (nAChRs) have been sought as novel therapeutics for nicotine cessation. $\alpha 4\beta 2$ nAChRs have been shown to be involved in mediating the addictive properties of nicotine while other subtypes (i.e., $\alpha 3\beta 4$ and $\alpha 7$) are believed to mediate the undesired effects of potential CNS drugs. To obtain selective molecules, it is important to understand the physicochemical features of ligands that affect selectivity and potency on nAChR subtypes. Here we present novel QSAR/QSSR models for negative allosteric modulators of human $\alpha 4\beta 2$ nAChRs and human $\alpha 3\beta 4$ nAChRs. These models support previous homology model and site-directed mutagenesis studies that suggest a novel mechanism of antagonism. Additionally, information from the models presented in this work was used to synthesize novel molecules; which subsequently led to the discovery of a new selective antagonist of human $\alpha 4\beta 2$ nAChRs.

© 2011 Elsevier Ltd. All rights reserved.

Neuronal nicotinic acetylcholine receptors (nAChRs) are ligand gated ion channels and members of the cys-loop family of receptors. nAChRs are found both in the peripheral and central nervous systems and are implicated in many diseases and disorders such as: Alzheimer's disease, epilepsy, autism, Parkinson's disease, depression, anxiety, and nicotine addiction.^{1,2} Worldwide, nicotine addiction is a significant problem. Smoking is the primary cause of preventable death worldwide and roughly 90% of the people who attempt to quit are unable to do so.³ It is now known that $\alpha 4\beta 2$ nAChRs are primarily responsible for the addiction to tobacco related products.^{4–6} Current FDA approved treatments for tobacco addiction are nicotine replacement, bupropion (Zyban[®]), and varenicline (Chantix[®]). Each of these therapies has a modest success of 20–30% abstinence 1 year after quit date.^{7,8} However, drugs such as varenicline have been associated with severe adverse cardiovascular effects.⁹ This combined with the low success rates of therapies warrant the need for novel small molecules that can be used in nicotine cessation. In an attempt to discover better therapeutics for nicotine cessation, some laboratories have proposed

non-competitive antagonists that target nAChRs.^{10,11} Mecamylamine, a non-selective non-competitive nAChR antagonist, was shown to promote 40% abstinence at the 1 year mark when used as an agonist–antagonist therapy in combination with the nicotine patch.¹⁰ In addition, Yoshimura et al. (2007)¹¹ discovered a novel negative allosteric modulator (NAM) that was selective for neuronal nAChRs as opposed to the muscle nAChR which significantly blocked nicotine self-administration on fixed and progressive ratio schedules in rats. These data support the use of non-competitive antagonists and NAMs as nicotine cessation therapies; however, to produce new therapeutic molecules it is believed that nAChR subtype selectivity must be pursued.¹²

Our laboratory has previously published the synthesis and pharmacology of a novel class of NAMs.^{13–19} We have previously reported a novel NAM, KAB-18, which shows selectivity for human $\alpha 4\beta 2$ (H $\alpha 4\beta 2$) nAChRs and through SAR have identified several chemical features important for its selectivity.¹⁹ One problem with the study of non-competitive and allosteric agents is the fact that most of these agents lack information concerning the site of interaction on their target receptor. To address this, we have constructed a homology model for the extracellular domain of the H $\alpha 4\beta 2$ nAChR and have identified the site in which these NAMs

* Corresponding author. Tel.: +1 614 330 1463.

E-mail address: mckay.2@osu.edu (B.J. Henderson).

interact allosterically through blind docking and molecular dynamics (MD) simulations.¹⁹ In this study, three-dimensional qualitative structure–activity relationship (3D-QSAR) studies and three-dimensional qualitative structure–selectivity relationship (3D-QSSR) studies were completed to study the relationship between functional activity (e.g., IC_{50} values) and selectivity of NAMs with their 3D structures. This study reports the construction and analysis of models that predict the detailed structural interactions of this novel class of NAMs^{18,19} with their binding site on $H\alpha 4\beta 2$ nAChRs and $H\alpha 3\beta 4$ nAChRs. In addition to this, we propose a model which distinguishes the physicochemical features that are important for selectivity for $H\alpha 4\beta 2$ nAChRs versus $H\alpha 3\beta 4$ nAChRs that also agree with previously reported homology modeling, SAR, and site-directed mutagenesis studies.^{19,23} Finally, these models were used in the generation of novel $H\alpha 4\beta 2$ nAChR antagonists.

To facilitate the presentation of data, four regions for the NAM scaffold have been defined (Fig. 1B). These four regions were defined from a pharmacophore model that was generated previously by using KAB-18 and KAB-18 like molecules.¹⁹ This pharmacophore model featured four hydrophobic regions and one hydrogen bond acceptor region. Region 1 was defined as the substitution on the nitrogen moiety of the piperidine ring containing hydrophobic domain 1 (Fig. 1B). Region 2 was defined as the ester acyl substitution containing the biphenyl (Fig. 1B). Region 3 was the piperidine ring which has been defined in the pharmacophore as the fourth hydrophobic region (Fig. 1B). Region 4 was the linkage between Regions 2 and 3, containing an ester bond with a hydrogen bond accepting domain (Fig. 1B). All of the NAMs presented in this manuscript contain one or more stereogenic centers. In construction of the QSAR and QSSR models the selected conformation of compounds used in the alignment play a pivotal role in determining the position of the field contribution maps and validation of the model. The conformation of our NAMs was determined by selecting the stereoisomers that match those found to be most stable in previously conducted docking and MD simulations on the $H\alpha 4\beta 2$ nAChR homology model.¹⁹ Enantiomers of NAMs at position C3 (respective of the piperidine ring, Region 3, Fig. 1B) have shown no functional difference in either $H\alpha 4\beta 2$ or $H\alpha 3\beta 4$ nAChRs.¹⁹ Choosing this set of conformations for NAMs in the QSAR and QSSR models allow the results to be compared to homology model data in addition to previous SAR data.¹⁹ The alignment of NAMs (Fig. 1A) and the construction of QSAR and QSSR ($H\alpha 4\beta 2/H\alpha 3\beta 4$) models using CoMSIA are described in detail in the Methods section (refer to Supplementary data). For every molecule used in the construction of the models, 3D structures were prepared and are also described in the Methods section. All functional data for training set molecules are detailed in Table 1 and the functional data for test set molecules are found in Table 2. Using

SYBYL's CoMSIA program, linear regression analyses were performed to correlate the experimentally derived pIC_{50} values with the computationally derived pIC_{50} values (Fig. S1). Fifty-five molecules were chosen for the $H\alpha 4\beta 2$ QSAR model training set and 42 molecules were chosen for the $H\alpha 4\beta 2$ QSAR and the QSSR models (Table 1). Correlation coefficients (r^2) for the $H\alpha 4\beta 2$ QSAR, $H\alpha 3\beta 4$ QSAR and QSSR models were 0.766, 0.761, and 0.871 respectively for the training set (Table 3, Fig. S1). Ten molecules were chosen for the test set for all molecules (Table 2). Correlation coefficients (r^2) for the $H\alpha 4\beta 2$ QSAR, $H\alpha 3\beta 4$ QSAR and QSSR models were 0.620, 0.621, and 0.480 respectively for the test set (Table 3, Fig. S1).

CoMSIA descriptors for steric (green/yellow field maps), electrostatic (blue/red field maps), hydrophobic (purple/gray field maps), hydrogen bond donor (cyan/magenta field maps), and hydrogen bond acceptors (orange/red field maps) were generated for the $H\alpha 4\beta 2$ QSAR, $H\alpha 3\beta 4$ QSAR, and QSSR models (Figs. 2–4, respectively). For detailed description of the model construction process, refer to the Methods section (see Supplementary data). KAB-18 was used as the structural scaffold for all field contribution maps (Figs. 2–4) due to its selectivity for $H\alpha 4\beta 2$ nAChRs.¹⁹

For the $H\alpha 4\beta 2$ nAChR QSAR model, steric contributions were important surrounding the phenyl rings of Regions 1 and 2 as well as the piperidine of Region 3 (Fig. 2A). Important electrostatic interactions were predicted surrounding the anthranilic moiety (positive) and the phenyl (negative) of Region 2 (Fig. 2B). Hydrophobic contributions were shown to be important around the phenyl rings of Regions 1 and 2 as well as the piperidine of Region 3 (Fig. 2C). Hydrophobic contributions were shown to be disfavored around the propyl chain of Region 1 (Fig. 2C). The protonated hydrogen of the piperidine nitrogen of Region 3 is predicted to act as a hydrogen bond donor (Fig. 2D) and the carbonyl of Region 4 is predicted to act as a hydrogen bond acceptor (Fig. 2E). These predictions support the binding mode of KAB-18 that has been recently presented by molecular dynamics (MD) simulation on the $H\alpha 4\beta 2$ nAChR homology model.¹⁹ This MD simulation predicted that the protonated hydrogen of the piperidine nitrogen is involved in a stabilizing hydrogen bond with the carbonyl group of Glu60 on the $\beta 2$ subunit.¹⁹ This agrees with the favored hydrogen bond donor predicted to occur in Region 3 by the $H\alpha 4\beta 2$ QSAR where the cyan field surrounds the piperidine nitrogen (Fig. 2D). The carbonyl of Region 4 was also shown to be involved in another important hydrogen bond with Thr58 on the $\beta 2$ subunit and this interaction was validated through site-directed mutagenesis.^{19,23} This agrees with the favored hydrogen bond acceptor predicted in Region 4 of the $H\alpha 4\beta 2$ QSAR where the orange field surrounds the carbonyl of KAB-18 (Fig. 2E). Additionally, the model predicts favorable interactions between negative electron densities of ligands in

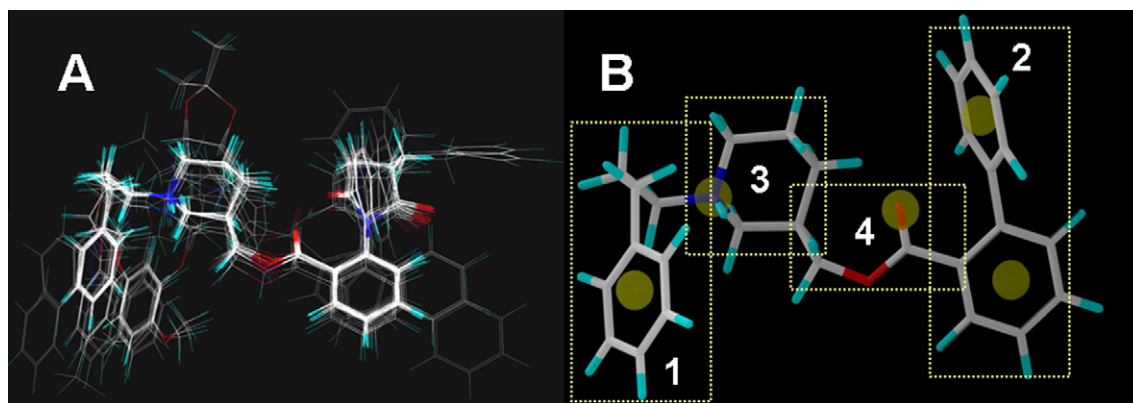


Figure 1. Alignment of the negative allosteric modulators. (A) Alignment of molecules used in QSAR and QSSR models (Figs. 2–4). (B) Regions of the NAM scaffold displayed with scaffold molecule, KAB-18.

Table 1
Observed and predicted IC₅₀ values of NAMs used in QSAR and QSSR models (training set molecules)

	Structure	QSAR (H α 4 β 2)		QSAR (H α 3 β 4)		QSSR (H α 4 β 2/H α 3 β 4)	
		Obs. pIC ₅₀ ^a	Pred. pIC ₅₀	Obs. pIC ₅₀ ^a	Pred. pIC ₅₀	Obs. [SI] ^a	Pred. [SI]
APB-1		4.99	4.96				
APB-10		5.00	4.86				
APB-4 ^b		4.84	4.75	4.81	4.87	0.02	-0.08
APB-8		4.84	4.86	4.65	4.13	0.19	0.79
COB-1 ^b		5.15	5.20	5.09	5.41	0.06	-0.19
COB-2 ^b		5.16	4.93	5.32	5.21	-0.16	-0.07
COB-3 ^b		5.62	5.67	5.19	4.82	0.43	0.73
COB-8		5.04	5.03	5.18	5.07	-0.14	-0.05
DDR-13 ^b		5.22	5.20	3.48	3.43	1.74	1.78

(continued on next page)

Table 1 (continued)

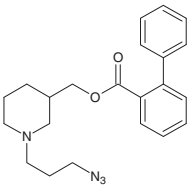
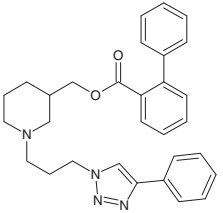
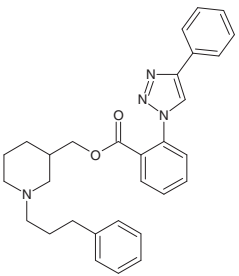
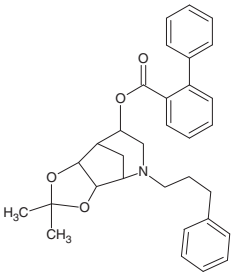
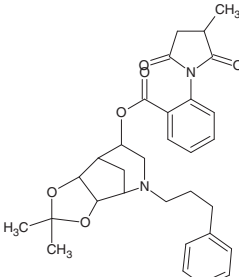
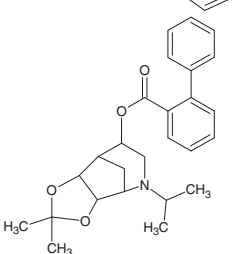
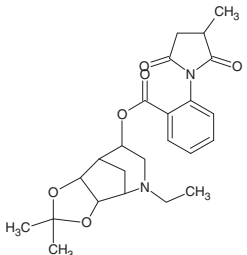
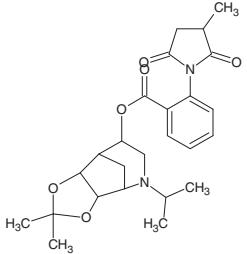
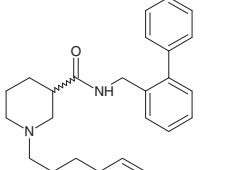
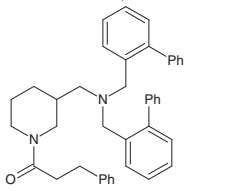
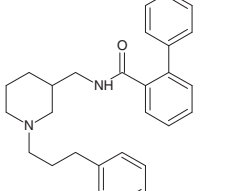
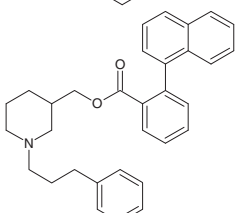
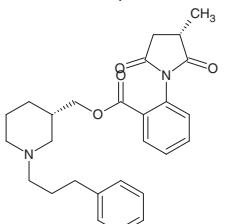
Structure	QSAR (H α 4 β 2)		QSAR (H α 3 β 4)		QSSR (H α 4 β 2/H α 3 β 4)	
	Obs. pIC ₅₀ ^a	Pred. pIC ₅₀	Obs. pIC ₅₀ ^a	Pred. pIC ₅₀	Obs. [SI] ^a	Pred. [SI]
	5.37	5.23	5.74	5.57	-0.38	-0.26
	5.19	5.32	3.41	3.36	1.78	1.97
	5.55	5.59	5.37	5.34	0.19	0.34
	4.94	4.89	4.86	3.64	0.08	1.07
	4.96	4.99	4.51	4.65	0.45	0.19
	5.02	5.00				

Table 1 (continued)

Structure	QSAR (H α 4 β 2)		QSAR (H α 3 β 4)		QSSR (H α 4 β 2/H α 3 β 4)	
	Obs. pIC ₅₀ ^a	Pred. pIC ₅₀	Obs. pIC ₅₀ ^a	Pred. pIC ₅₀	Obs. [SI] ^a	Pred. [SI]
 <chem>CN1CCOC1COC2=CN(C)C=O2C3=CC=CC=C3</chem>	4.92	5.06	4.11	4.66	0.81	0.15
 <chem>CN1CCOC1COC2=CN(C)C=O2C3=CC=CC=C3C4(C)C</chem>	5.12	5.05				
 <chem>O=C(NC1=CC=C(C=C1)C2=CC=CC=C2)CC1CCN(C1)CCC3=CC=CC=C3</chem>	4.78	4.80	4.84	5.14	-0.06	-0.54
 <chem>CC1=CC=C(C=C1)C(=O)N2CCN(C2C3=CC=CC=C3)CC4=CC=CC=C4</chem>	4.68	4.64	4.39	4.55	0.29	-0.05
 <chem>O=C(NC1=CC=C(C=C1)C2=CC=CC=C2)CC1CCN(C1)CCC3=CC=CC=C3</chem>	4.70	4.66	1.00	0.68	3.70	4.00
 <chem>COC1=CC=C(C=C1)C2=CC=CC=C2C3=CC=CC=C3OCC4CCN(C4)CCC5=CC=CC=C5</chem>	4.93	5.04	4.2	3.75	0.73	1.29
 <chem>CN1CCOC1COC2=CN(C)C=O2C3=CC=CC=C3</chem>	4.98	5.15	4.96	4.84	0.02	0.31

(continued on next page)

Table 1 (continued)

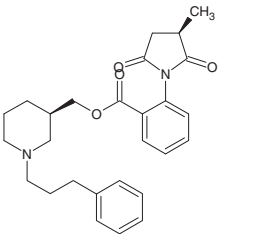
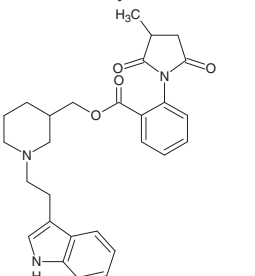
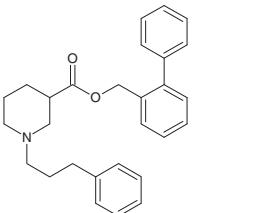
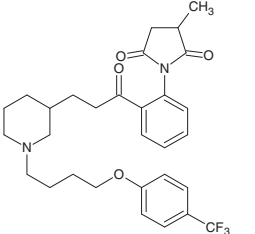
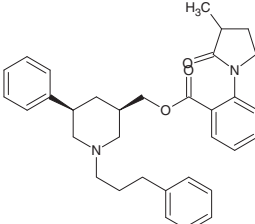
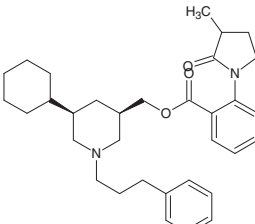
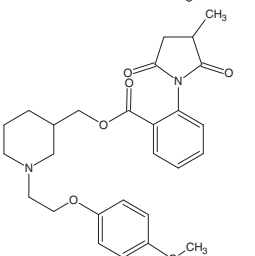
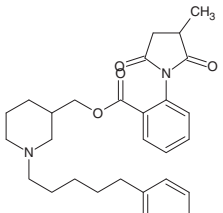
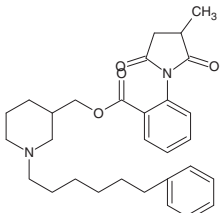
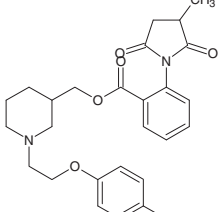
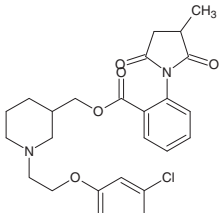
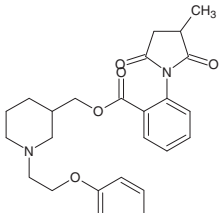
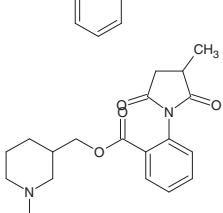
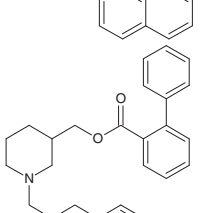
Structure	QSAR (H α 4 β 2)		QSAR (H α 3 β 4)		QSSR (H α 4 β 2/H α 3 β 4)	
	Obs. pIC ₅₀ ^a	Pred. pIC ₅₀	Obs. pIC ₅₀ ^a	Pred. pIC ₅₀	Obs. [SI] ^a	Pred. [SI]
 IB-4 ^b	5.05	5.15	5.02	4.84	0.02	0.31
 JHB-7	5.25	5.36	4.13	4.13	1.12	1.18
 JHB-9 ^b	4.75	4.86	4.99	5.01	0.24	-0.35
 JHB-11	5.15	5.24				
 JHB-12	5.27	4.99				
 JHB-13	4.40	4.53	4.07	4.09	0.33	0.24
 KAB-9	4.18	4.39	4.92	4.60	-0.75	-0.32

Table 1 (continued)

Structure	QSAR (H α 4 β 2)		QSAR (H α 3 β 4)		QSSR (H α 4 β 2/H α 3 β 4)	
	Obs. pIC ₅₀ ^a	Pred. pIC ₅₀	Obs. pIC ₅₀ ^a	Pred. pIC ₅₀	Obs. [SI] ^a	Pred. [SI]
	4.61	5.01	5.38	4.94	-0.77	-0.08
	4.53	4.60				
	4.95	4.80	4.73	4.97	0.22	-0.04
	4.66	4.70	4.94	4.90	0.14	0.11
	5.41	5.26	4.80	4.73	0.61	0.55
	5.13	5.05	5.17	5.18	-0.04	-0.06
	4.87	5.03	1.00	1.73	3.87	3.30

(continued on next page)

Table 1 (continued)

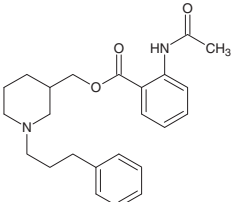
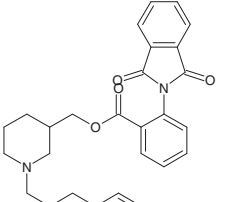
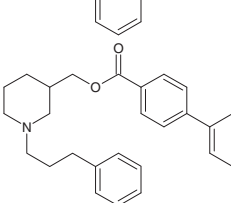
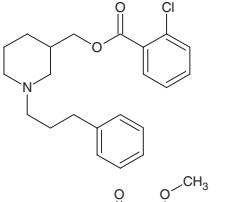
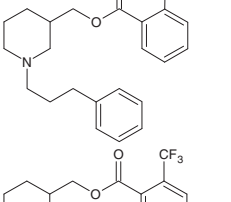
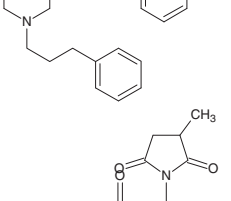
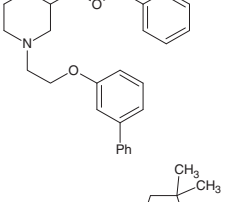
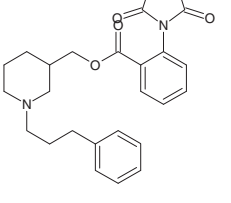
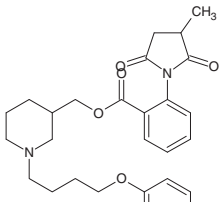
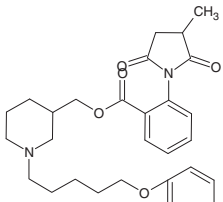
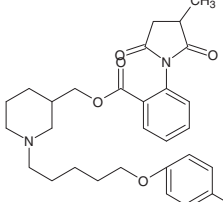
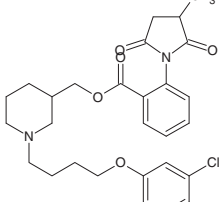
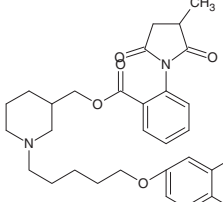
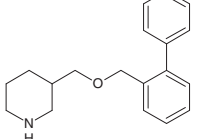
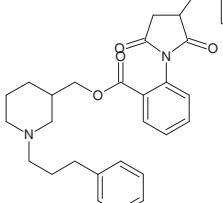
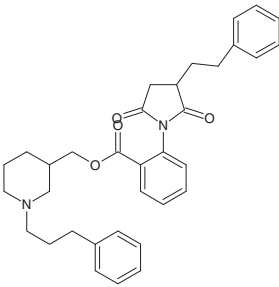
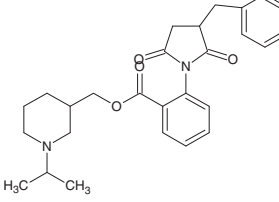
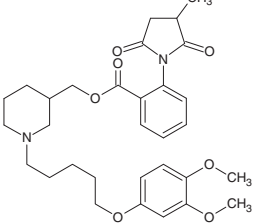
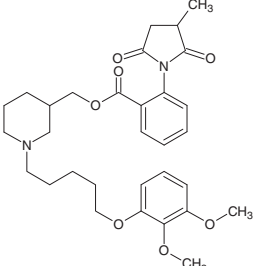
Structure	QSAR (H α 4 β 2)		QSAR (H α 3 β 4)		QSSR (H α 4 β 2/H α 3 β 4)	
	Obs. pIC ₅₀ ^a	Pred. pIC ₅₀	Obs. pIC ₅₀ ^a	Pred. pIC ₅₀	Obs. [SI] ^a	Pred. [SI]
	5.26	5.31	5.37	5.42	-0.11	0.04
	5.30	5.22	5.23	5.13	0.07	0.05
	5.20	5.14	4.73	4.79	0.47	0.43
	5.03	5.11	4.64	4.74	0.39	0.34
	5.10	5.26	4.92	4.93	0.19	0.34
	5.10	5.14	5.26	4.71	-0.16	0.37
	5.14	5.24	4.57	4.78	0.57	0.44
	5.31	5.26	5.30	5.17	0.01	0.07

Table 1 (continued)

Structure	QSAR (H α 4 β 2)		QSAR (H α 3 β 4)		QSSR (H α 4 β 2/H α 3 β 4)	
	Obs. pIC ₅₀ ^a	Pred. pIC ₅₀	Obs. pIC ₅₀ ^a	Pred. pIC ₅₀	Obs. [SI] ^a	Pred. [SI]
	5.77	5.24				
	4.77	4.75				
	4.84	4.84				
	4.91	5.09	4.13	4.22	0.78	0.56
	4.76	4.63	5.04	4.76	-0.28	-0.03
	5.38	5.29				
	4.97	4.96	4.84	4.81	0.14	0.23

(continued on next page)

Table 1 (continued)

Structure	QSAR (H α 4 β 2)		QSAR (H α 3 β 4)		QSSR (H α 4 β 2/H α 3 β 4)	
	Obs. pIC ₅₀ ^a	Pred. pIC ₅₀	Obs. pIC ₅₀ ^a	Pred. pIC ₅₀	Obs. [SI] ^a	Pred. [SI]
	5.29	5.22	4.48	4.71	0.81	0.58
	5.05	5.11				
	5.08	4.92	2.70	3.10	2.38	1.89
	5.06	4.93				

^a -Log of geometric mean, $n = 4-10$.^b Previously reported by Henderson et al.¹⁹Table 2
Observed and predicted IC₅₀ values of NAMs used in QSAR and QSSR models (test set molecules)

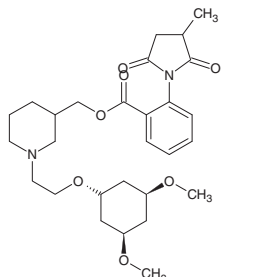
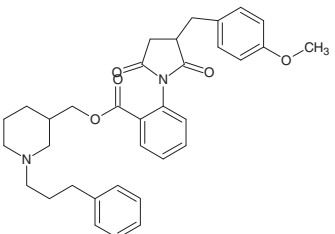
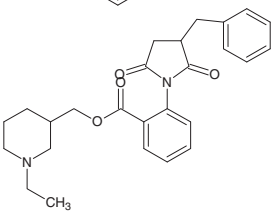
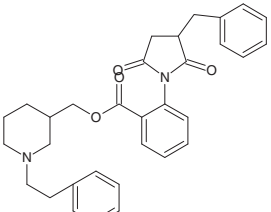
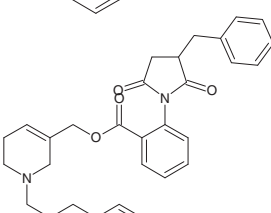
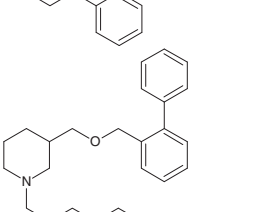
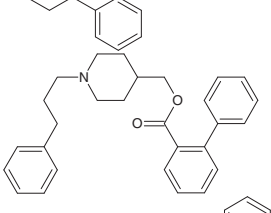
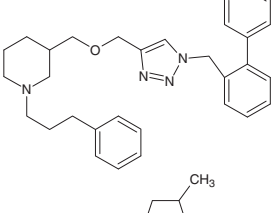
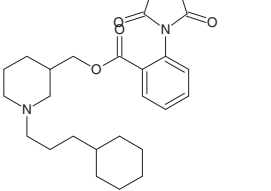
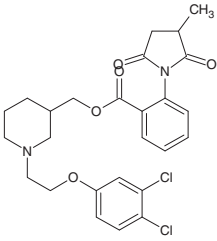
Structure	QSAR (H α 4 β 2)		QSAR (H α 3 β 4)		QSSR (H α 4 β 2/H α 3 β 4)	
	Obs. pIC ₅₀ ^a	Pred. pIC ₅₀	Obs. pIC ₅₀ ^a	Pred. pIC ₅₀	Obs. [SI] ^a	Pred. [SI]
	4.90	5.02	4.38	4.32	0.68	0.82

Table 2 (continued)

Structure	QSAR (H α 4 β 2)		QSAR (H α 3 β 4)		QSSR (H α 4 β 2/H α 3 β 4)	
	Obs. pIC ₅₀ ^a	Pred. pIC ₅₀	Obs. pIC ₅₀ ^a	Pred. pIC ₅₀	Obs. [SI] ^a	Pred. [SI]
 <chem>COC1=CC=C(C=C1)C2=CN(C2=O)C(=O)OCCCN3CCCCC3</chem>	4.41	4.87	4.54	4.66	-0.13	-0.28
 <chem>C1=CC=C(C=C1)C2=CN(C2=O)C(=O)OCCCN3CCCCC3</chem>	5.35	5.12	4.93	4.55	0.42	0.29
 <chem>C1=CC=C(C=C1)C2=CN(C2=O)C(=O)OCCCN3CCCCC3</chem>	5.35	5.24	4.93	4.78	0.42	0.51
 <chem>C1=CC=C(C=C1)C2=CN(C2=O)C(=O)OCCCN3CCCCC3</chem>	5.29	5.35	5.43	4.99	-0.14	-0.44
 <chem>C1=CC=C(C=C1)C2=CN(C2=O)C(=O)OCCCN3CCCCC3</chem>	4.90	4.85	4.81	4.38	0.09	0.35
 <chem>C1=CC=C(C=C1)C2=CN(C2=O)C(=O)OCCCN3CCCCC3</chem>	5.09	5.00	4.98	5.05	0.11	0.65
 <chem>C1=CC=C(C=C1)C2=CN(C2=O)C(=O)OCCCN3CCCCC3</chem>	5.54	5.17	5.14	5.10	0.39	0.13
 <chem>CC1=CNC(=O)C1=OCCCN2CCCCC2</chem>	4.84	5.03	4.97	4.75	-0.14	0.26

(continued on next page)

Table 2 (continued)

Structure	QSAR (H α 4 β 2)		QSAR (H α 3 β 4)		QSSR (H α 4 β 2/H α 3 β 4)	
	Obs. pIC ₅₀ ^a	Pred. pIC ₅₀	Obs. pIC ₅₀ ^a	Pred. pIC ₅₀	Obs. [SI] ^a	Pred. [SI]
 KAB-14	4.82	4.95	4.76	4.81	0.06	-0.01

^a -Log of geometric mean, $n = 4-10$.

Table 3
QSAR and QSSR analysis results

Dependent variable	Data set		
	QSAR (H α 4 β 2)	QSAR (H α 3 β 4)	QSSR
r^2 (training set)	0.856	0.761	0.871
standard error	0.15	0.57	0.57
F value	26.13	15.1	14.3
Components	6	6	6
r^2 (test set)	0.620	0.621	0.480

Region 1 (Fig. 2B). This has been observed previously with an analog of KAB-18 that included a carbonyl in Region 1,¹⁹ which lead to a 3-fold increase in potency for H α 4 β 2 nAChRs.

The H α 3 β 4 nAChR QSAR model predicted that steric features in both Regions 1 and 2 had a positive effect on potency (Fig. 3A). Electrostatic field maps predicted that negative electrostatics contribute to potency in Region 1 and positive electrostatics contribute to potency in Region 2 (Fig. 3B). Hydrophobic features were shown to be disfavored in Regions 1 and 2 (Fig. 3C). Hydrogen bond donors were shown to be favorable with the piperidine of Region 3 and the propyl chain in Region 1 (Fig. 3D). Hydrogen bond acceptors in

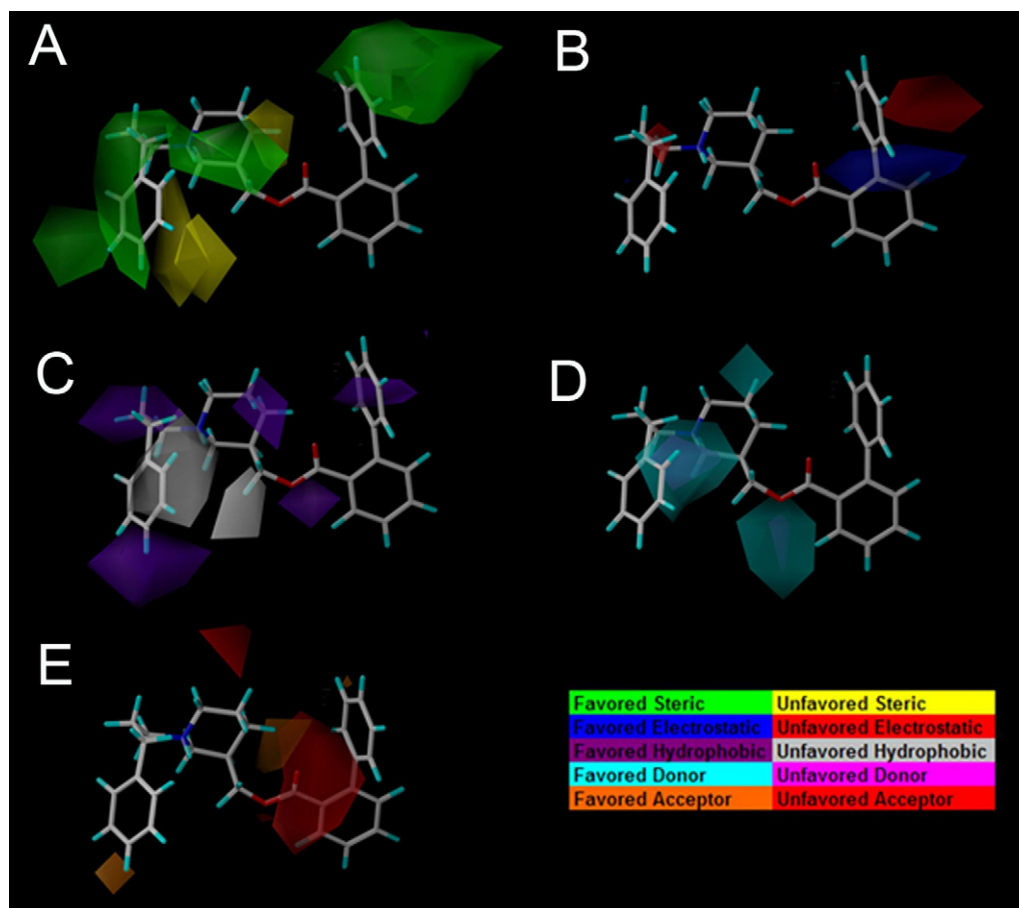


Figure 2. CoMSIA models for H α 4 β 2 nAChRs. Steric (A), electrostatic (B), hydrophobic (C), hydrogen bond donor (D), and hydrogen bond acceptor (E) field contribution maps are shown with KAB-18. Bottom right, color key to field contribution maps. Greater potency (lower IC₅₀ values) is correlated with: less bulk near yellow/gray, more bulk near green/purple, more hydrogen bond acceptors near blue/red, less hydrogen bond acceptors near red, More hydrogen bond donors near cyan and less hydrogen bond donors near magenta.

Region 4 were shown to be unfavorable around the carbonyl of Region 4 and favorable with the phenyl of Region 2 (Fig. 3E). One feature that supports findings from previous SAR data,¹⁹ concerns aromatic-containing features in Regions 1 and 2 (e.g., phenylpropyl substitution in Region 1) that contribute to a decrease of potency on H α 3 β 4 nAChRs. This agrees with the disfavored hydrophobics that are predicted by the H α 3 β 4 QSAR where the gray fields surround the phenylpropyl of KAB-18 (Fig. 3C). One finding that differs significantly between the H α 4 β 2 and H α 3 β 4 QSAR is in the lack of a favored hydrogen bond acceptor in Region 3 of the H α 3 β 4 QSAR (Fig. 3D). Also, the hydrophobics and hydrogen bond acceptor field maps are opposing when compared between the H α 4 β 2 and H α 3 β 4 QSAR models (Figs. 2C, E and 3C, E). Altogether, this suggests that this class of NAMs may have significantly different binding interactions between H α 4 β 2 and H α 3 β 4 nAChRs.

The QSSR model predicted that steric interactions are important for selectivity on H α 4 β 2 nAChRs surrounding the phenyl rings of Regions 1, 2, and 3 (Fig. 4). The field contribution maps also showed that sterics surrounding the propyl chain of Region 1 decrease selectivity (Fig. 4A). Thus, the net effect of removing steric contributions in Region 1 may lead to an increase in selectivity. Electrostatic field maps predicted that positive electrostatics in Regions 1 (around the phenylpropyl of KAB-18) and 4 (ester Region of KAB-18) contribute to selectivity for H α 4 β 2 nAChRs while negative electrostatics near Region 2 (biphenyl of KAB-18) decrease selectivity (Fig. 4B). Hydrophobic maps predicted that hydrophobic features in Regions 1, 2, and 3 (piperidine region of KAB-18),

specifically at the phenyl ring positions, contribute to selectivity for H α 4 β 2 nAChRs while hydrophobics in Region 4 decrease selectivity (Fig. 4C). Donor contribution maps predicted that Hydrogen bond donors in Region 4 contribute to selectivity on H α 4 β 2 nAChRs (Fig. 4D). Acceptor maps predicted that hydrogen bond acceptors are favored in Region 4 surrounding the ester carbonyl of (Fig. 4E). Many of these findings predicted by the QSSR model support findings of our previous SAR data.¹⁹ As mentioned earlier, the presence of aromatic containing features in both Regions 1 and 2 were shown to be important for the selectivity on H α 4 β 2 nAChRs. The predictions of the steric and hydrophobic QSSR field contribution maps, which show both green and purple fields surrounding KAB-18's phenylpropyl (Region 1) and phenyl group (Region 2), support this (Fig. 4A and C). As mentioned earlier, SAR data supported the importance of the specific orientation of the carbonyl in Region 4. The acceptor field contribution maps support this finding as well as the favored HBA field (orange field) surrounds the carbonyl group of KAB-18. This suggests that the atom acceptor's placement (flanking the biphenyl of Region 2) is important for selectivity (Fig. 4E). Many of the features highlighted in this QSSR model correlate blind docking and MD simulation studies with an H α 4 β 2 nAChR homology model.¹⁹ The regions shown to be important in the QSSR model overlap with amino acid residues that have been proposed to interact with KAB-18 (i.e., Phe118 in Region 1 and Thr58 in Region 4 [both on β 2 subunit]). These residues are not conserved in the H α 3 β 4 nAChR and may be important for mediating selectivity for H α 4 β 2 nAChRs. Previous SAR studies¹⁹

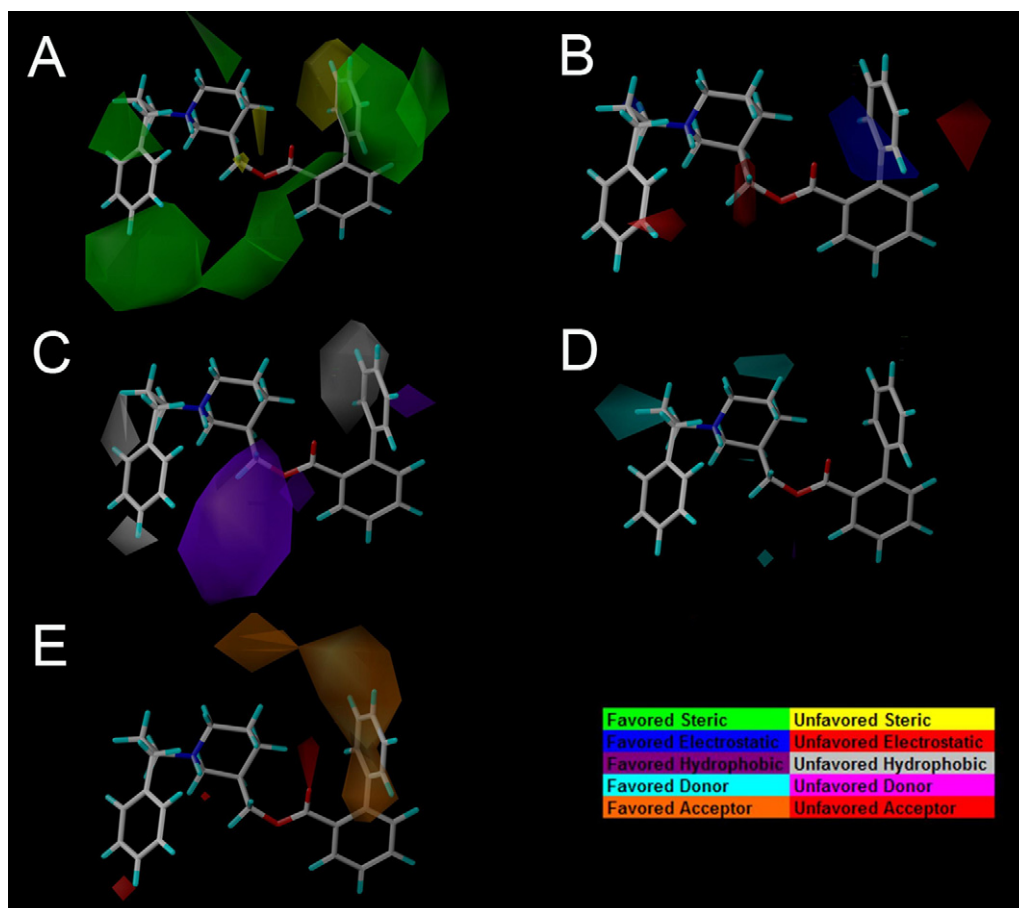


Figure 3. CoMSIA models for H α 3 β 4 nAChRs. Steric (A), electrostatic (B), hydrophobic (C), hydrogen bond donor (D), and hydrogen bond acceptor (E) field contribution maps are shown with KAB-18. Bottom right, color key to field contribution maps. Greater potency (lower IC₅₀ values) is correlated with: less bulk near yellow/gray, more bulk near green/purple, more hydrogen bond acceptors near blue/red, less hydrogen bond acceptors near red, More hydrogen bond donors near cyan and less hydrogen bond donors near magenta.

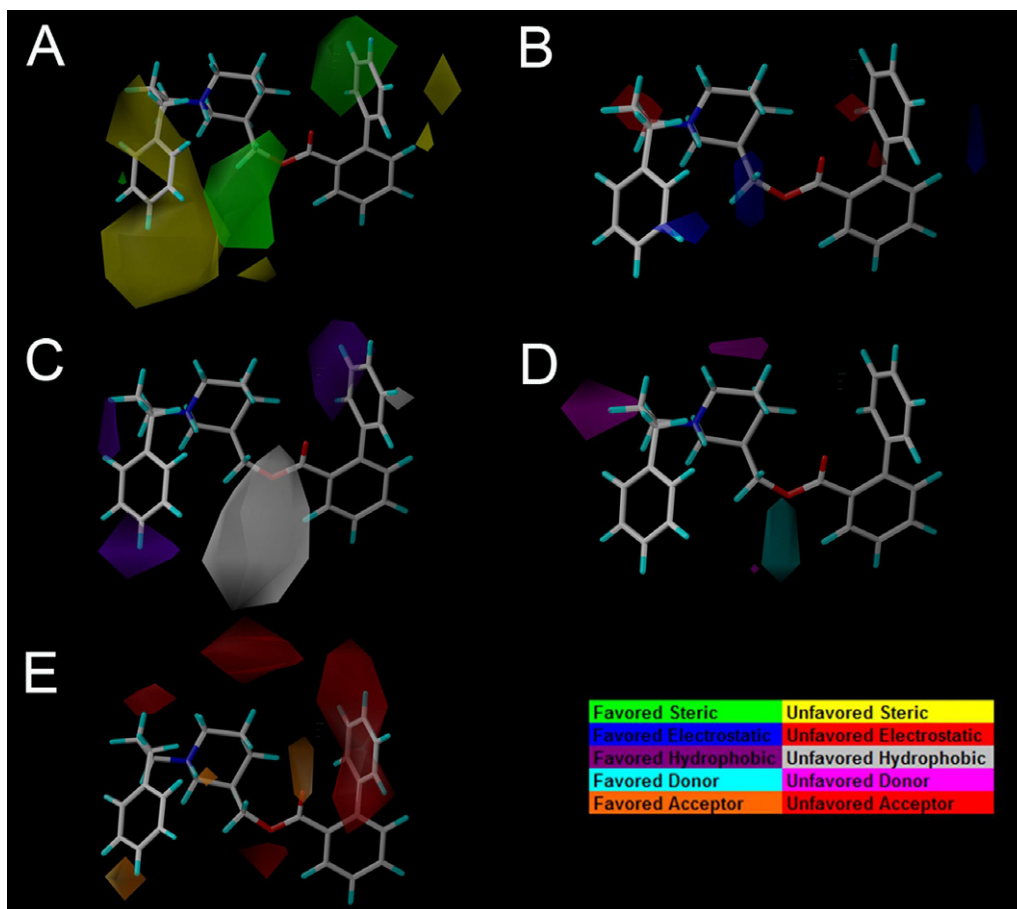
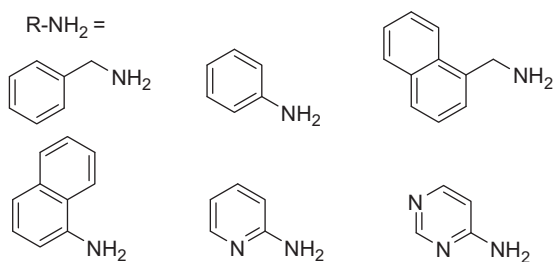
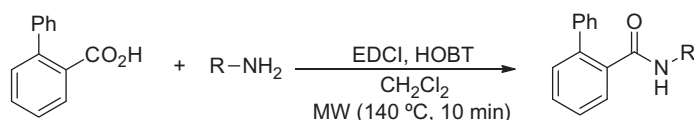


Figure 4. 3D-QSSR CoMSIA models of NAMs. Steric (A), electrostatic (B), hydrophobic (C), hydrogen bond donor (D), and hydrogen bond acceptor (E) field contribution maps are shown with KAB-18. Bottom right, color key to field contribution maps. Greater selectivity (more potent on H α 4 β 2 vs H α 3 β 4) is correlated with: less bulk near yellow/gray, more bulk near green/purple, more hydrogen bond acceptors near blue/red, less hydrogen bond acceptors near red, More hydrogen bond donors near cyan and less hydrogen bond donors near magenta.



Scheme 1. Synthesis of novel biphenyl amides.

molecules that have improved potency on H α 4 β 2 nAChRs; but still preserve selectivity for H α 4 β 2 nAChRs. Novel molecules were synthesized (Scheme 1) and tested for inhibitory activity on both H α 4 β 2 and H α 3 β 4 nAChRs (Table 4).



Two molecules (COB-170 and COB-171) were found to be 2-fold more potent than lead molecule, KAB-18. The phenylmethyl analog (COB-170) had an IC₅₀ of 7.5 and 8.5 μ M on H α 4 β 2 and H α 3 β 4 nAChRs, respectively (Table 4). The phenyl analog (COB-171) had an IC₅₀ of 6.9 and 10.7 μ M on H α 4 β 2 and H α 3 β 4 nAChRs, respectively (Table 4). The naphthylmethyl (COB-172) produced no change in potency on H α 4 β 2 nAChRs (IC₅₀ value, 13.9 μ M, Table 4); but maintained selectivity for H α 4 β 2 nAChRs. The pyridinyl analog (COB-173) had an IC₅₀ value of 13.6 and 20.0 μ M on H α 4 β 2 and H α 3 β 4 nAChRs, respectively (Table 4). The pyrimidinyl analog (COB-174) had an IC₅₀ value of 25.1 and 39.6 μ M on H α 4 β 2 and H α 3 β 4 nAChRs, respectively (Table 4). Finally the naphthyl analog (COB-175) had an IC₅₀ value of 10.7 and 18.2 μ M on H α 4 β 2 and H α 3 β 4 nAChRs, respectively (Table 4). Concerning selectivity for H α 4 β 2 nAChRs over H α 3 β 4 nAChRs, COB-170, COB-171, COB-173, and COB-174 are all nonselective

have identified three regions of importance for the selectivity of NAMs on H α 4 β 2 nAChRs: (1) The phenyl in Region 2; (2) the placement of the carbonyl group in Region 4; and (3) the presence of an aromatic feature in Region 1. When the aromatic feature is removed from Region 1, a loss of selectivity is observed; however, these molecules show an increase in potency up to 5-fold.¹⁹ This is supported by the H α 4 β 2 nAChR QSAR model (Fig. 2C). The QSSR model also predicted that hydrophobic features were important for H α 4 β 2 selectivity in Regions 1 and 3 (Fig. 4C) while steric features in Region 1 may decrease selectivity for H α 4 β 2 nAChRs (Fig. 4A). Therefore, increasing the hydrophobics in Region 3 may improve selectivity for H α 4 β 2 nAChRs. We hypothesized that by combining these two findings (incorporating reduced sterics in Region 1 and increased hydrophobics in Region 3) we would obtain

Table 4
Inhibition of new antagonists on H α 4 β 2 and H α 3 β 4 nAChRs

	R	H α 4 β 2 nAChRs			H α 3 β 4 nAChRs		
		IC ₅₀ value ^a (μ M)	n_H ^b		IC ₅₀ value ^a (μ M)	n_H ^b	F_m ^c
COB-170		7.5 (6.1–9.2)	–1.1	7.6 (6.4–9.0)	–1.8	1.0	
COB-171		6.9 (5.8–8.2)	–1.3	10.7 (8.4–13.6)	–2.2	1.6	
COB-172		13.9 (6.1–31.6)	–0.7	>100 ^d	–0.4	>10	
COB-173		13.6 (12.0–15.5)	–1.0	17.5 (10.7–28.4)	–0.9	1.3	
COB-174		25.1 (19.9–31.7)	–1.5	39.6 (36.1–43.6)	–0.9	1.6	
COB-175		10.7 (8.3–13.8)	–0.8	18.2 (9.9–33.5)	–1.2	1.8	

^a Values represent geometric means (confidence limits), $n = 3–7$.

^b n_H , Hill coefficient.

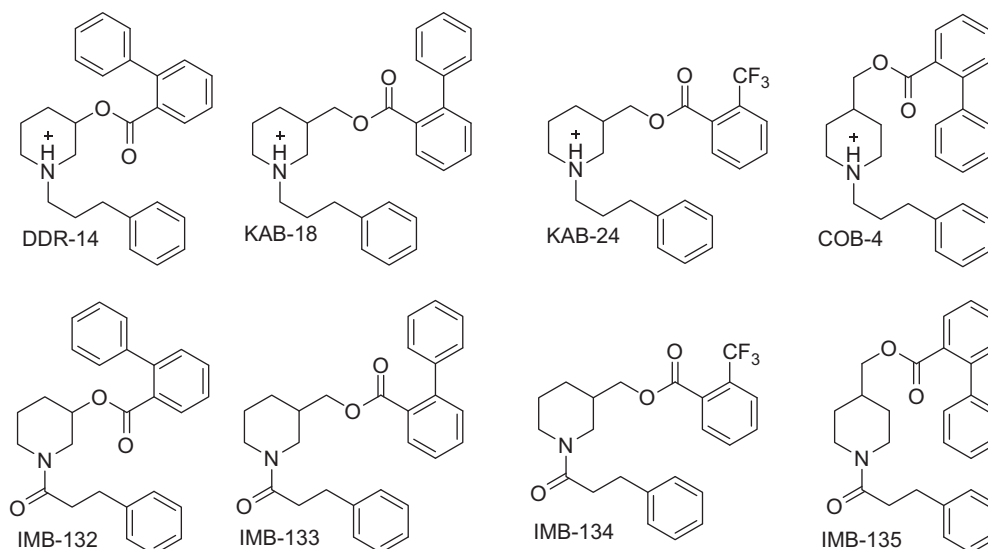
^c Fold difference in potency H α 3 β 4/H α 4 β 2.

^d No activity up to concentrations of 100 μ M.

(Table 4). COB-175 showed a 2-fold preference for H α 4 β 2 nAChRs (Table 4). The methylnaphthyl analog (COB-172) is as potent and selective as lead molecule, KAB-18.

The H α 4 β 2 nAChR QSAR model shows that negative electronics contribute to potency near the piperidine moiety of Region 3 contribute to potency (Fig. 2B). This is also supported by previous data that shows the addition of an amide group leads to an increase in potency.¹⁹ To determine the importance of this finding, several new molecules (IMB-132, IMB-133, IMB-134, IMB-135) containing amide groups in Region 1 were made from scaffolds that have been previously reported¹⁹ (KAB-18, DDR-14, KAB-24, COB-4) (Scheme 2).

The new amide-containing molecules (IMB-132, IMB-133, IMB-134, IMB-135) were all more potent than their original scaffolds (DDR-14, KAB-18, KAB-24, COB-4) on H α 4 β 2 nAChRs (Table 5). IMB-132 resulted in a 1.5-fold increase in potency on H α 4 β 2 nAChRs (IC₅₀ value, 2.7 μ M, Table 5). IMB-134 resulted in a 2.1-fold increase in potency on H α 4 β 2 nAChRs (IC₅₀ value, 3.9 μ M, Table 5). IMB-135 resulted in a 1.4 increase in potency on H α 4 β 2 nAChRs (IC₅₀ value, 5.9 μ M, Table 5). Finally, IMB-133 resulted in a 2.4-fold increase in potency on H α 4 β 2 nAChRs (IC₅₀ value, 5.7 μ M, Table 5). IMB-132 showed a 2-fold decrease in potency on H α 3 β 4 nAChRs compared to its scaffold molecule, DDR-14 (IC₅₀ value 6.3 μ M, Table 5). IMB-133, IMB-134, and



Scheme 2. Novel compounds containing amide functionality in Region 1 and previously reported scaffolds. Synthetic details have been previously described.^{13,16,20–22}

Table 5
Inhibition of new antagonists on $\text{H}\alpha 4\beta 2$ and $\text{H}\alpha 3\beta 4$ nAChRs

	$\text{H}\alpha 4\beta 2$ nAChRs		$\text{H}\alpha 3\beta 4$ nAChRs		
	IC ₅₀ value (μM) ^a	n_{H} ^b	IC ₅₀ value (μM) ^a	n_{H} ^b	F _m ^c
IMB-132	4.3 (2.2–8.5)	–1.6	6.0 (4.3–8.3)	–1.6	1.5
DDR-14 ^d	6.5 (4.1–10.4)	–1.6	2.7 (0.4–17.9)	–1.4	
IMB-133	5.6 (3.6–9.0)	–0.9	>100 ^e	~	2.4
KAB-18 ^d	13.5 (9.7–18.5)	–1.4	>100 ^e	~	
IMB-134	3.9 (3.3–4.8)	–1.5	6.3 (5.4–7.3)	–2.1	2.1
KAB-24 ^d	8.0 (4.2–15.3)	–0.8	5.5 (1.7–17.4)	–0.8	
IMB-135	5.9 (5.2–6.7)	–1.2	9.4 (7.4–11.9)	–1.5	1.4
COB-4 ^d	8.1 (2.1–30.7)	–0.8	10.5 (7.6–14.4)	–1.0	

^a Values represent geometric means (confidence limits), $n = 3$ –5.

^b n_{H} , Hill coefficient.

^c Fold difference in potency carbonyl/non-carbonyl.

^d Previously reported data.¹⁹

^e No activity up to concentrations of 100 μM .

IMB-135 showed no change in potency on $\text{H}\alpha 3\beta 4$ nAChRs compared to its scaffolds (KAB-18, KAB-24, COB-4, respectively).

The QSAR and QSSR models presented here describe the physicochemical interactions that are important for potency on $\text{H}\alpha 4\beta 2$ and $\text{H}\alpha 3\beta 4$ nAChRs as well as selectivity for $\text{H}\alpha 4\beta 2$ nAChRs versus $\text{H}\alpha 3\beta 4$ nAChRs. The fact that these models agree with previously reported modeling and functional data support their strength and validity. With the models presented here combined with the information gathered from previous SAR, homology modeling, and site directed mutagenesis, there are many physicochemical features identified in this scaffold that mediate $\text{H}\alpha 4\beta 2$ nAChR selectivity. These include steric/hydrophobic features in both Regions 1 and 2 as well as a hydrogen bond acceptor in Region 4. Previous SAR has highlighted the importance of aromatic rings in Regions 1 and 2; but these models suggest that aromatics may not be necessary to preserve potency or selectivity on $\text{H}\alpha 4\beta 2$ nAChRs. If true, this allows for additional flexibility in the design of novel scaffolds. However, this will need to be confirmed by designing and synthesizing novel molecules containing distinct hydrophobic and steric features as opposed to aromatic features to determine how this will affect potency and selectivity. Previous SAR also points to the importance of the carbonyl group in Region 4. The QSAR and QSSR models suggest the importance of this position lies in the role as a hydrogen bond acceptor. This finding correlates with the docking studies that show a stable hydrogen bond between Thr58 of the $\beta 2$ subunit and the carbonyl group in KAB-18's Region 4.^{19,23} There may be potential at this position for increasing selectivity by placing a feature that will enable stronger hydrogen bonding with Thr58 ($\beta 2$ subunit). Most importantly, this finding suggests that maintaining an acceptor atom at this position is significant for both potency and selectivity and should be remain in the design of future molecules. The $\text{H}\alpha 4\beta 2$ nAChR QSAR model suggests that the following changes will increase potency on $\text{H}\alpha 4\beta 2$ nAChRs: (1) increasing electronegative character in Region 2's anthranilic moiety, (2) increasing the electropositive character in the area surrounding Region 2's phenyl ring, and (3) addition of a hydrogen bond donor in Regions 2 and 4. This $\text{H}\alpha 4\beta 2$ QSAR model also suggests that a hydrogen bond donor in Region 3 is important for potency on $\text{H}\alpha 4\beta 2$ nAChRs. This agrees with previous modeling studies where the hydrogen of the piperidine nitrogen in Region 3 forms a stable hydrogen bond with Glu60 of the $\beta 2$ subunit.^{19,23}

Using these QSAR and QSSR models, new molecules were synthesized. According to the QSAR and QSSR models, the new COB series were designed to: (1) enhance potency by reducing the unfavored sterics in Region 1 and (2) maintain selectivity by increasing favored hydrophobics in Region 3. The new IMB compounds were designed to increase potency by increasing the favorable electrostatics predicted in Regions 1 and 3. Of the new COB molecules,

two of the six showed a higher preference for $\text{H}\alpha 4\beta 2$ nAChRs over $\text{H}\alpha 3\beta 4$ nAChRs (Table 4). Two molecules (COB-170 and COB-171) were found to be 2-fold more potent than lead molecule, KAB-18. The naphthylmethyl (COB-172) maintained potency on $\text{H}\alpha 4\beta 2$ nAChRs and also maintained selectivity for $\text{H}\alpha 4\beta 2$ nAChRs (Table 4). This can be considered a significant improvement, as COB-172's scaffold is more 'drug like' when compared to KAB-18 (Table S1); but is still selective for $\text{H}\alpha 4\beta 2$ nAChRs. The novel synthesis of the IMB compounds also shows strong evidence that inclusion of amide groups may improve potency to a small degree; but does so consistently. Altogether, this work presents novel QSAR and QSSR models for nAChRs. These models present important chemical features for a novel class of NAMS that promote both selectivity and potency on $\text{H}\alpha 4\beta 2$ nAChRs. Finally, these models have aided in the design and synthesis of potent, novel antagonists of $\text{H}\alpha 4\beta 2$ and $\text{H}\alpha 3\beta 4$ nAChRs as well as the discovery of a new, drug-like, selective antagonist of $\text{H}\alpha 4\beta 2$ nAChRs (COB-172).

Acknowledgments

All stably-transfected human cell lines were kindly provided by Dr. Jon M. Lindstrom, Department of Neuroscience School of Medicine, University of Pennsylvania, Philadelphia, PA. This work was supported by the National Institutes of Health National Institute on Drug Abuse [Grant DA029433]. Financial support for B.J.H. is from the National Institutes of Health National Institute on Drug Abuse Diversity Supplement. We also want to thank Phil Cruz of Tripos for his help in providing technical support on SYBYL 7.1 features and applications.

Supplementary data

Supplementary data associated with this article can be found, in the online version, at doi:10.1016/j.bmcl.2011.11.051.

References and notes

- Lloyd, G. K.; Williams, M. J. *Pharmacol. Exp. Ther.* **2000**, 292, 461.
- Gotti, C.; Zoli, M.; Clementi, F. *Trends Pharmacol. Sci.* **2006**, 27, 482.
- Knight, C.; Howard, P.; Baker, C. L.; Marton, J. P. *Value Health* **2009**, 13, 209.
- Tapper, A. R.; McKinney, S. L.; Nashmi, R.; Schwarz, J.; Deshpande, P.; Labarca, C.; Whiteaker, P.; Marks, M. J.; Collins, A. C.; Lester, H. A. *Science* **2004**, 306, 1029.
- Lester, H. A.; Fonck, C.; Tapper, A. R.; McKinney, S.; Damaj, M. I.; Balogh, S.; Owens, J.; Wehner, J. M.; Collins, A. C.; Labarca, C. *Curr. Opin. Drug Discov. Devel.* **2003**, 6, 633.
- Piccioletto, M. R.; Zoli, M.; Rimondini, R.; Léna, C.; Marubio, L. M.; Pich, E. M.; Fuxe, K.; Changeux, J.-P. *Nature* **1998**, 391, 173.
- Mihalak, K. B.; Carroll, F. I.; Luetje, C. W. *Mol. Pharmacol.* **2006**, 70, 801.
- Rollema, H.; Chambers, L. K.; Coe, J. W.; Glowa, J.; Hurst, R. S.; Lebel, L. A.; Lu, Y.; Mansbach, R. S.; Mather, R. J.; Rovetti, C. C.; Sands, S. B.; Schaeffer, E.; Schulz, D. W.; Tingley, F. D.; Williams, K. E. *Neuropharmacol.* **2007**, 52, 985.
- Singh, S.; Loke, Y. K.; Spangler, J. G.; Furberg, C. D. *Can. Med. Ass. J.* **2011**. doi:10.1503/cmaj.110218.
- Rose, J. E.; Behm, F. M.; Westman, A. C.; Evin, E. D.; Tein, R. M.; Ripka, G. V. *Clin. Pharmacol. Ther.* **1994**, 56, 86.
- Yoshimura, R. F.; Hogenkamp, D. J.; Li, W. Y.; Tran, M. B.; Belluzzi, J. D.; Whittemore, E. R.; Leslie, F. M.; Gee, K. W. *J. Pharmacol. Exp. Ther.* **2007**, 323, 907.
- Jensen, A. A.; Frolund, B.; Liljefors, T.; Krogsgaard-Larsen, P. J. *Med. Chem.* **2005**, 48, 4705.
- Bergmeier, S. C.; Lapinsky, D. J.; Free, R. B.; McKay, D. B. *Bioorg. Med. Chem. Lett.* **1999**, 9, 2263.
- Bryant, D. L.; Free, R. B.; Thomasy, S. M.; Lapinsky, D. J.; Ismail, K. A.; McKay, S. B.; Bergmeier, S. C.; McKay, D. B. *Neurosci. Res.* **2002**, 42, 57.
- Bryant, D. L.; Free, R. B.; Thomasy, S. M.; Lapinsky, D. J.; Ismail, K. A.; Arason, K. M.; Bergmeier, S. C.; McKay, D. B. *Ann. N. Y. Acad. Sci.* **2002**, 971, 139.
- Bergmeier, S. C.; Ismail, K. A.; Arason, K. M.; McKay, S.; Bryant, D. L.; McKay, D. B. *Bioorg. Med. Chem. Lett.* **2004**, 14, 3739.
- Huang, J.; Orac, C. M.; McKay, S.; McKay, D. B.; Bergmeier, S. C. *Bioorg. Med. Chem.* **2008**, 16, 3816.
- González-Cestari, T. F.; Henderson, B. J.; Pavlovic, R. E.; McKay, S. B.; El Hajj, R. A.; Pulipaka, A. B.; Orac, C. M.; Reed, D. D.; Boyd, R. T.; Zhu, M. X.; Li, C.; Bergmeier, S. C.; McKay, D. B. *J. Pharmacol. Exp. Ther.* **2009**, 328, 504.

19. Henderson, B. J.; Pavlovicz, R. E.; Allen, J. D.; Gonzalez-Cestari, T. F.; Orac, C. M.; Bonnel, A. B.; Zhu, M. X.; Boyd, R. T.; Li, C.; Bergmeier, S. C.; McKay, D. B. *J. Pharmacol. Exp. Ther.* **2010**, 334, 761.
20. Bergmeier, S. C.; Ismail, K. A. *Synthesis* **2000**, 2000, 1369.
21. Ismail, K. A.; Bergmeier, S. C. *Eur. J. Med. Chem.* **2002**, 37, 469.
22. Arason, K. M.; Bergmeier, S. C. *Org. Prep. Proc. Int.* **2001**, 34, 337.
23. Pavlovicz, R.E.; Henderson, B.J.; Bonnell, A.B.; Boyd, R.T.; and McKay, D.B.; Li, C. PLoS ONE 6: e24949. doi:10.1371/journal.pone.0024949.